NASA TECHNICAL MEMORANDUM

NASA TM X- 73,161

NASA TM X-73,161

ELEMENTARY APPLICATIONS OF A ROTORCRAFT DYNAMIC STABILITY ANALYSIS

Wayne Johnson

Ames Research Center

and

Ames Directorate
U.S. Army Air Mobility R&D Laboratory
Moffett Field, Calif. 94035

June 1976

1. Report No.	2. Government Accession No.	3. Recipient's Catalog No.
NASA TM X-73,161		

4. Title and Subtitle	5. Report Date
ELEMENTARY APPLICATIONS OF A ROTORCRAFT DYNAMIC STABILITY ANALYSIS	6. Performing Organization Code

7. Author(s)	8. Performing Organization Report No.
Wayne Johnson	A-6717
	10. Work Unit No. 505-10-22
9. Performing Organization Name and Address NASA Ames Research Center and Ames Directorate, U.S. Army Air Mobility R&D Laboratory, Moffett Field, Calif. 94035	11. Contract or Grant No.
	13. Type of Report and Period Covered Technical Memorandum
12. Sponsoring Agency Name and Address National Aeronautics and Space Administration, Washington, D.C. 20546 and U.S. Army Air Mobility R&D Laboratory, Moffett Field, California 94035	14. Sponsoring Agency Code

15. Supplementary Notes

16. Abstract

A number of applications of a rotorcraft aeroelastic analysis are presented, intended to verify that the analysis encompasses the classical solutions of rotor dynamics, and to examine the influence of certain features of the model. Results are given for the following topics: flapping frequency response to pitch control; forward flight flapping stability; pitch/flap flutter and divergence; ground resonance instability; and the flight dynamics of several representative helicopters.

17. Key Words (Suggested by Author(s))	18. Distribution Statement
Rotor dynamics Helicopter flying qualities	Unlimited STAR Category - 01

19. Security Classif. (of this report)	20. Security Classif. (of this page)	21. No. of Pages	22. Price*
Unclassified	Unclassified	24	$3.25

*For sale by the National Technical Information Service, Springfield, Virginia 22161

NOMENCLATURE

c	rotor blade chord
C_T	rotor thrust coefficient
C_ζ	Rotor lag damping coefficient
I_b	rotor blade flapping moment of inertia
I_p	rotor blade pitch moment of inertia
R	rotor radius
$t_{\frac{1}{2}}$	time to half amplitude of mode (seconds)
t_2	time to double amplitude of mode (seconds)
T	period of mode (seconds)
V	forward speed
x_A/c	distance blade section aerodynamic center is aft of the pitch axis (fraction of chord)
x_I/c	distance blade section center of gravity is aft of the pitch axis (fraction of chord)
γ	blade Lock number
ζ	damping ratio of a root
λ	eigenvalue or root of a mode (dimensionless, based on the rotor rotational speed)
μ	rotor advance ratio, forward speed divided by tip speed
ν_β	flap natural frequency in rotating frame (per rev)
ν_ζ	blade lag rotating natural frequency (per rev)
σ	rotor solidity ratio
ω_θ	natural frequency of blade pitch motion (per rev)
Ω	rotor rotational speed

ELEMENTARY APPLICATIONS OF A ROTORCRAFT DYNAMIC STABILITY ANALYSIS

Wayne Johnson*

Ames Research Center
and
Ames Directorate
U.S. Army Air Mobility R&D Laboratory

SUMMARY

A number of applications of a rotorcraft aeroelastic analysis are presented, intended to verify that the analysis encompasses the classical solutions of rotor dynamics, and to examine the influence of certain features of the model. Results are given for the following topics: flapping frequency response to pitch control; forward flight flapping stability; pitch/flap flutter and divergence; ground resonance instability; and the flight dynamics of several representative helicopters.

INTRODUCTION

An aeroelastic analysis has been developed for rotorcraft, applicable to isolated rotor, rotor with wind tunnel support, and complete helicopter dynamics. The analysis is described in reference 1. This report presents a number of examples of the dynamic behavior calculated using this aeroelastic model. The first purpose of these applications is to check out the sophisticated analysis by demonstrating that it encompasses several elementary, classical solutions in rotor dynamics. The second purpose is to examine the influence on the dynamics of some features available in the model.

RESULTS AND DISCUSSION

Flapping Frequency Response

Figures 1 to 3 present the frequency response of a three-bladed rotor in hover to pitch control inputs. Figure 1 shows the coning response to

*Research Scientist, Large Scale Aerodynamics Branch.

collective inputs for an articulated rotor ($\nu = 1$ and $\gamma = 8$). Figures 2 and 3 show respectively the lateral and longitudinal tip-path-plane tilt response to lateral cyclic input for a hingeless rotor ($\nu = 1.15$ and $\gamma = 8$). Three cases are shown: with no inflow dynamics, with a quasistatic inflow dynamics model, and with the complete inflow dynamics model. The difference between the quasistatic and complete inflow dynamics models is simply that the latter includes a first order time lag in the inflow response to rotor force perturbations (see reference 1). The influence of the rotor inflow on both the steady and high frequency response can be significant, but the quasistatic model gives nearly the same results as the complete inflow dynamics model (c.f. references 2 and 3).

Forward Flight Flapping Stability

Figure 4 presents a root locus of the flapping stability of an articulated rotor blade in forward flight ($\nu = 1$ and $\gamma = 10$). The blade motion consists of the rigid flap degree of freedom, with no shaft motion. The analysis is for a single blade in the rotating system, including the influence of the periodic coefficients on the dynamic stability. This result, including the advance ratio at the stability boundary, compares well with simpler solutions (c.f. references 4 and 5). The roots were calculated using a step size of $\Delta\Psi = 12^\circ$ in the integration of the equations of motion (over one period, for use in the Floquet theory analysis). This azimuth increment is really more appropriate for a three- or four-bladed rotor; for a single blade at high advance ratio a step size of $\Delta\Psi = 1$ or 2° gives more accurate results.

Pitch/Flap Flutter

Next consider the pitch/flap flutter of an articulated rotor blade ($\nu = 1$ and $\gamma = 8$). The degrees of freedom involved are rigid flap and rigid pitch motion, with the pitch bearing outboard of the flap hinge. The following values are used for the rotor chord (fraction of rotor radius), pitch inertia (fraction of flapping inertia), and rotor thrust coefficient to solidity ratio: $c/R = 0.1$, $I_p/I_b = 0.001$, and $C_T/\sigma = 0.07$. The flutter and divergence boundaries are plotted in figures 5 to 7, as the control system stiffness (i.e. the pitch natural frequency ω_θ) required for stability as a function of the chordwise center of gravity/aerodynamic

center offset. A large enough control system stiffness or forward center of gravity position stabilizes both the divergence and flutter modes. Figure 5 presents the pitch/flap flutter boundaries for the hovering articulated rotor with aerodynamic center offsets $x_A = 0$ and .05c. This result compares well with the classical solutions (see reference 6). Figure 6 shows the effect of adding the first flapwise bending mode (with natural frequency 2.6/rev) to the analysis, for the hovering rotor with $x_A = 0$. Finally figure 7 shows the influence of forward flight on the flutter boundaries, for advance ratios $\mu = 0$ and $\mu = 0.3$. The $\mu = .3$ results are based on a constant coefficient approximation, using the average of the coefficients in the rotating frame; it is better to make this approximation in the nonrotating frame however, for a rotor with several blades.

Ground Resonance

Now we shall consider some results from ground resonance investigations. Ground resonance is a mechanical instability involving the inplane motion of the rotor hub due to flexibility of the helicopter or wind tunnel support, coupled with the rotor cyclic lag degrees of freedom (see reference 7). For a specific rotor support system, the ground resonance stability boundary may be expressed in terms of the lag damping required to stabilize the motion. Deutsch (reference 8) developed a simple criterion for the lag damping required for stability, based on the assumption that the blade mass is small compared with the support mass (which is almost always true). Figure 8 presents a comparison of the ground resonance stability boundary calculated using the dynamics analysis of reference 1, with the results of the Deutsch criterion. The points are for two full-scale rotors on a number of wind tunnel support configurations; the line represents exact agreement of the two calculations. The correlation is very good.

Figure 9 presents the ground resonance stability calculated for a hovering, four-bladed articulated rotor in a wind tunnel. The rotor and the support properties for this case are given in table 1. The analysis

used the rigid flap and lag degrees of freedom for each blade, and two longitudinal and two lateral degrees of freedom for the hub support. The figure shows the damping ratio of the four support modes as a function of rotor speed, for three levels of blade lag damping (C_ζ). Each support mode is stabilized at the resonance with the high frequency lag mode -- $\omega_{support} = (1 + \nu_\zeta)\Omega$; and at a higher rotor speed a degradation in stability occurs due to the resonance with the low frequency lag mode -- $\omega_{support} = (1 - \nu_\zeta)\Omega$. With low enough lag damping it is the latter resonance which produces the ground resonance instability. In general the mode which goes unstable in this resonance (i.e. the support mode or the lag mode) depends on which has the least uncoupled damping. In the root locus it is the mode nearest the imaginary axis which actually makes the excursion into the right-half-plane as the rotor speed is varied. In the example of figure 9, the lateral balance mode has a low level of damping (table 1), so at resonance the support mode damping decreases while there is a corresponding increase in the damping of the low frequency lag mode. For well damped support modes, the ground resonance instability will occur at such low lag damping that it is the lag mode which actually goes into the right-half-plane (a mode involving both rotor and support motion of course).

Helicopter Flight Dynamics

The rotorcraft aeroelastic analysis of reference 1 has also been applied to the calculation of helicopter flight dynamics. Tables 1 to 5 present typical results. Four aircraft are considered: a small articulated rotor helicopter (gross weight 1160 kg, rotor radius 4.0 m), a large articulated rotor helicopter (gross weight 15200 kg, rotor radius 11.0 m), a soft-inplane hingeless rotor helicopter (gross weight 2100 kg, rotor radius 4.9 m), and a tandem rotor helicopter (gross weight 8600 kg, rotor radius 7.6 m). The tables give the period and damping for the flight dynamics modes in hover and in forward flight at 100 knots. The basic model has three rigid body degrees of freedom (uncoupled lateral or longitudinal motions) plus the rotor flapping degrees of freedom. The roots for the basic model are compared with results using a quasistatic approximation for the rotor flap dynamics; including the rotor lag degrees of freedom;

including the rotor inflow perturbation (unsteady aerodynamics); and with results including all six rigid body degrees of freedom (coupled longitudinal and lateral dynamics). For the soft-inplane hingeless rotor (table 4), the results including both rotor lag and rotor torsion degrees of freedom are also presented. For the tandem rotor helicopter (table 5), the basic model includes the rotor inflow perturbation, since rotor-rotor interference has an important role in the dynamics. See references 9 and 10 for discussions of the modes represented by the eigenvalues given in tables 2 to 5.

Generally it is concluded from the data in tables 2 to 5 that the quasistatic approximation is very good; that the inflow perturbation has a significant, and sometimes very important influence on the flight dynamics; and that the assumption of separate longitudinal and lateral motions is not usually valid, at least in terms of the eigenvalues. Rotor lag motion and other degrees of freedom may be required in the model; this is particularly true for the hingeless rotor, where the degrees of freedom have a large influence on the dynamics.

CONCLUDING REMARKS

A comprehensive analysis of rotorcraft aeroelastic behavior (reference 1) has been applied to a number of classical problems in rotor dynamics. The results presented agree well with the solutions available in the literature. The satisfactory treatment of the classical problems such as these is a basic prerequisite for any analysis which is to be applied to the more complex problems of rotorcraft dynamics. In addition, it has been possible to examine the influence of a number of features of the analytical mode, including the effect of inflow perturbations on rotor flap response and helicopter flight dynamics, the characteristics of the ground resonance instability, and the role of the rotor degrees of freedom in helicopter flight dynamics.

REFERENCES

1. Johnson, Wayne, "Aeroelastic Analysis for Rotorcraft in Flight or in a Wind Tunnel," NASA TN-D, in preparation

2. Peters, David A., "Hingeless Rotor Frequency Response with Unsteady Inflow," NASA SP-352, February 1974

3. Ormiston, Robert A., and Peters, David A., "Hingeless Helicopter Rotor Response with Nonuniform Inflow and Elastic Blade Bending," J. Aircraft, 9, 10, October 1972

4. Horvay, Gabriel, "Rotor Blade Flapping Motion," Quarterly of Applied Mathematics, 5, 2, July 1947

5. Johnson, Wayne, "Perturbation Solutions for the Influence of Forward Flight on Helicopter Rotor Flapping Stability," NASA TM X-62361, August 1974

6. Miller, R.H., and Ellis, C.W., "Helicopter Blade Vibration and Flutter," Journal of the American Helicopter Society, 1, 3, July 1956

7. Coleman, Robert P., and Feingold, Arnold M., "Theory of Self-Excited Mechanical Oscillations of Helicopter Rotors with Hinged Blades," NACA Report 1351, 1958

8. Deutsch, M.L., "Ground Vibrations of Helicopter," Journal of the Aeronautical Sciences, 13, 5, May 1946

9. Gessow, Alfred and Myers, Garry C., Aerodynamics of the Helicopter, Frederick Ungar Publishing Co., New York, 1952

10. Seckel, Edward, Stability and Control of Airplanes and Helicopters, Academic Press, New York, 1964

Table 1. Rotor and support parameters for the ground resonance calculations of figure 9.

Rotor:

Radius	5.3 m
Number of blades	4
Hinge offset (% radius)	5.9
Lag frequency, ν_ζ (per rev)	.31
Blade mass	46.3 kg
Blade first moment of inertia	116 kg-m
Blade second moment of inertia	381 kg-m^2

Support:

mode	natural frequency Hz	modal mass kg	modal damping N/m/sec
long. balance	1.76	27000	36500
lat. balance	2.16	11000	6900
long. strut	3.04	24500	38000
lat. strut	3.68	18000	36500

Table 2. Small Articulated Rotor Helicopter Flight Dynamics

A. Hover

	Longitudinal modes				Lateral modes			
	T	t_2	$t_{\frac{1}{2}}$	$t_{\frac{1}{2}}$	T	t_2	$t_{\frac{1}{2}}$	$t_{\frac{1}{2}}$
1. Basic model	12.90	3.97	.769	.903	11.32	9.93	.388	1.137
2. Quasistatic rotor model	12.90	4.00	.777	.913	11.35	10.00	.399	1.144
3. Including rotor lag motion	12.90	3.95	.769	.900	11.36	10.14	.386	1.166
4. Including inflow perturbation	12.90	3.96	1.170	.893	11.12	9.30	.403	1.238
5. Coupled longitudinal and lateral dynamics	15.49	1.957	.700	.816	7.82	$t_{\frac{1}{2}} = 15.34$	$T = 19.33$ $t_{\frac{1}{2}} = .600$	

B. V = 100 knots

	Longitudinal modes				Lateral modes			
	T	$t_{\frac{1}{2}}$	T	$t_{\frac{1}{2}}$	T	$t_{\frac{1}{2}}$	T	$t_{\frac{1}{2}}$
1. Basic model	31.41	15.65	2.32	.608	20.30	2.06	1.552	.484
2. Quasistatic rotor model	31.42	15.55	2.34	.619	20.31	2.07	1.558	.484
3. Including rotor lag motion	31.41	15.71	2.32	.610	24.01	1.92	1.563	.494
4. Including inflow perturbation	32.70	14.71	2.37	.645	20.38	2.03	1.582	.501
5. Coupled longitudinal and lateral dynamics	30.86	34.39	2.26	.610	20.21	1.91	1.562	.487

Table 3. Large Articulated Rotor Helicopter Flight Dynamics

A. Hover

	Longitudinal modes				Lateral modes			
	T	t_2	$t_{\frac{1}{2}}$	$t_{\frac{1}{2}}$	T	t_2	$t_{\frac{1}{2}}$	$t_{\frac{1}{2}}$
1. Basic model	19.93	5.43	.535	1.544	11.30	10.78	.381	2.23
2. Quasistatic rotor model	19.86	5.47	.591	1.549	11.23	10.79	.391	2.27
3. Including rotor lag motion	19.90	5.38	.522	1.519	11.51	10.72	.379	2.13
4. Including inflow perturbation	19.92	5.41	1.074	1.547	11.07	18.32	.436	2.67
5. Coupled longitudinal and lateral dynamics	23.33	4.17	.564	1.372	9.34	$t_{\frac{1}{2}}$ = 7.83	.371	2.35

B. V = 100 knots

	Longitudinal modes				Lateral modes			
	T	t_2	$t_{\frac{1}{2}}$	$t_{\frac{1}{2}}$	T	$t_{\frac{1}{2}}$	$t_{\frac{1}{2}}$	$t_{\frac{1}{2}}$
1. Basic model	33.80	5.37	.373	2.72	3.57	1.099	.625	5.54
2. Quasistatic rotor model	33.52	5.40	.408	2.75	3.60	1.118	.610	5.57
3. Including rotor lag motion	34.36	5.37	.370	2.70	3.57	1.143	.586	6.58
4. Including inflow perturbation	34.78	5.23	.471	2.88	3.81	1.326	.607	5.58
5. Coupled longitudinal and lateral dynamics	40.71	5.68	T = 19.32 $t_{\frac{1}{2}}$ = .471		3.63	1.166	T = 48.43 $t_{\frac{1}{2}}$ = 3.38	

Table 4. Soft-Inplane Hingeless Rotor Helicopter Flight Dynamics

A. Hover

	Longitudinal modes				Lateral modes			
	T	t_2	$t_{\frac{1}{2}}$	$t_{\frac{1}{2}}$	T	$t_{\frac{1}{2}}$	$t_{\frac{1}{2}}$	t_2
1. Basic model	17.04	4.21	.639	1.393	5.99	3.81	.339	1.228
2. Quasistatic rotor model	17.03	4.23	.648	1.398	6.03	3.79	.340	1.233
3. Including rotor lag motion	17.06	4.20	.638	1.336	5.99	3.69	.339	1.232
4. Including rotor lag and torsion motion	17.07	3.65	.783	2.30	5.33	$t_2 = 16.48$	.374	.939
5. Including inflow perturbation	17.95	6.28	1.087	1.087	7.12	3.44	.233	1.366
6. Coupled longitudinal and lateral dynamics	23.56	3.65	.661	1.726	6.05	2.84	.354	1.609

B. V = 100 knots

	Longitudinal modes				Lateral modes			
	T	$t_{\frac{1}{2}}$	T	$t_{\frac{1}{2}}$	T	$t_{\frac{1}{2}}$	$t_{\frac{1}{2}}$	t_2
1. Basic model	63.19	19.16	3.38	.777	1.859	.785	.611	7.62
2. Quasistatic rotor model	63.23	19.09	3.40	.794	1.856	.781	.630	7.65
3. Including rotor lag motion	63.49	19.28	3.37	.776	1.861	.792	.602	7.50
4. Including rotor lag and torsion motion	36.30	15.34	3.02	1.128	1.785	.724	$T = 21.65$ $t_{\frac{1}{2}} = 16.94$	
5. Including inflow perturbation	70.92	18.60	3.33	.848	1.910	.822	.569	8.34
6. Coupled longitudinal and lateral dynamics	254.3	$t_2 = 13.89$	3.42	.863	1.852	.773	.549	$t_{\frac{1}{2}} = 9.78$

Table 5. Tandem Rotor Helicopter Flight Dynamics

A. Hover

	Longitudinal modes				Lateral modes			
	T	t_2	$t_{\frac{1}{2}}$	$t_{\frac{1}{2}}$	T	t_2	$t_{\frac{1}{2}}$	$t_{\frac{1}{2}}$
1. Basic model	25.04	27.37	.675	1.155	12.78	4.75	.759	15.01
2. Quasistatic rotor model	25.06	27.62	.691	1.172	12.74	4.82	.766	15.02
3. Including rotor lag motion	24.99	27.10	.671	1.152	12.78	4.70	.750	14.89
4. Without inflow perturbation	26.15	51.25	.463	.720	12.78	4.75	.759	14.37
5. Coupled longitudinal and lateral dynamics	25.06	11.97	.640	1.155	12.78	4.72	.776	8.75

B. V = 50 knots

	Longitudinal modes				Lateral modes			
	T	t_2	$t_{\frac{1}{2}}$	$t_{\frac{1}{2}}$	T	t_2	$t_{\frac{1}{2}}$	$t_{\frac{1}{2}}$
1. Basic model	26.40	4.00	.322	3.15	10.49	6.86	.713	9.17
2. Quasistatic rotor model	26.31	4.00	.341	3.16	10.54	6.84	.716	9.20
3. Including rotor lag motion	26.17	4.00	.331	3.13	10.24	5.38	.768	10.46
4. Without inflow perturbation	27.43	98.[illegible]	.447	.711	10.47	6.83	.714	9.31
5. Coupled longitudinal and lateral dynamics	29.13	3.83	.322	3.19	10.62	5.23	.711	4.23

Table 5. Concluded.

C. V = 100 knots

	Longitudinal modes				Lateral modes			
	T	t_2	$t_{\frac{1}{2}}$	$t_{\frac{1}{2}}$	T	t_2	$t_{\frac{1}{2}}$	$t_{\frac{1}{2}}$
1. Basic model	34.05	2.85	.267	3.04	15.07	7.11	1.295	1.295
2. Quasistatic rotor model	33.94	2.84	.284	3.05	15.15	6.36	1.130	1.422
3. Including rotor lag motion	33.75	2.82	.271	3.01	11.12	3.88	.937	4.97
4. Without inflow perturbation	25.48	21.73	.346	1.071	15.05	7.15	1.298	1.298
5. Coupled longitudinal and lateral dynamics	12.91	2.10	.266	3.35	48.62	4.36	T = 15.94 $t_{\frac{1}{2}}$ = 1.001	

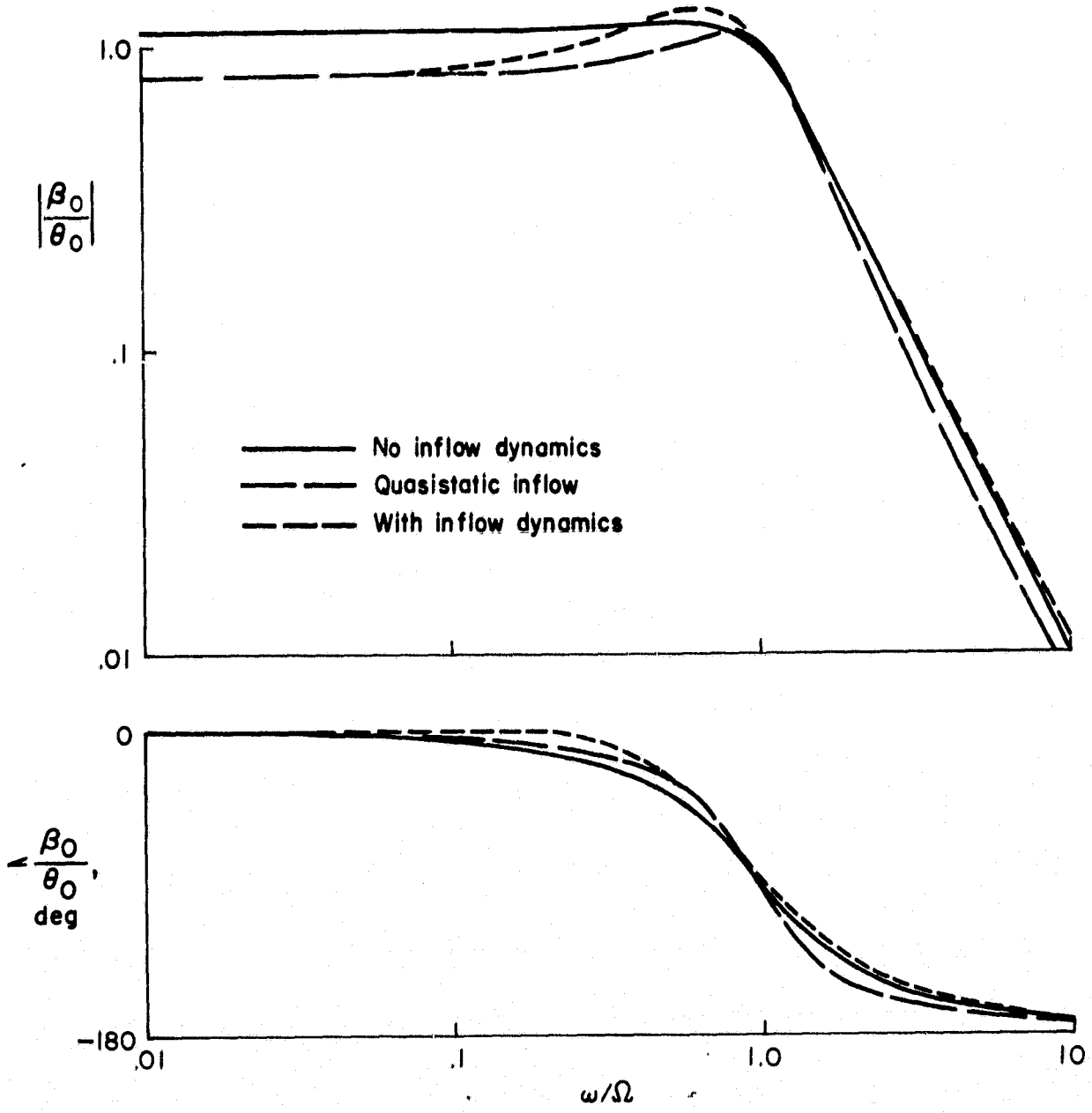

Figure 1. Magnitude and phase of coning response to collective inputs (β_0/θ_0) for a hovering, three-bladed articulated rotor (flap frequency $\nu = 1.0$), showing the influence of the inflow dynamics.

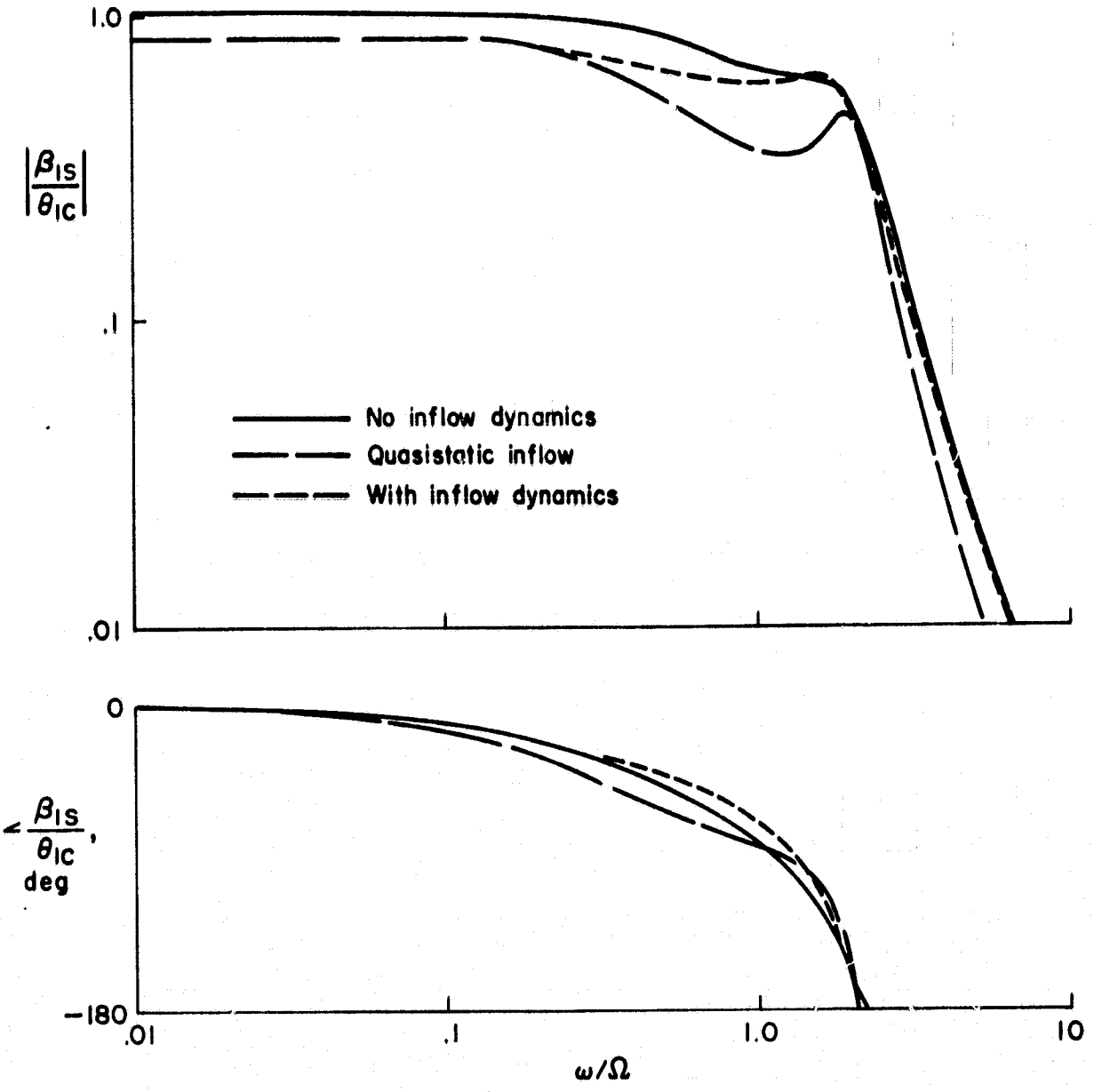

Figure 2. Magnitude and phase of lateral tip-path-plane tilt response to lateral control plane inputs (β_{1S}/θ_{1C}) for a hovering, three-bladed hingeless rotor (flap frequency $\nu = 1.15$), showing the influence of the inflow dynamics.

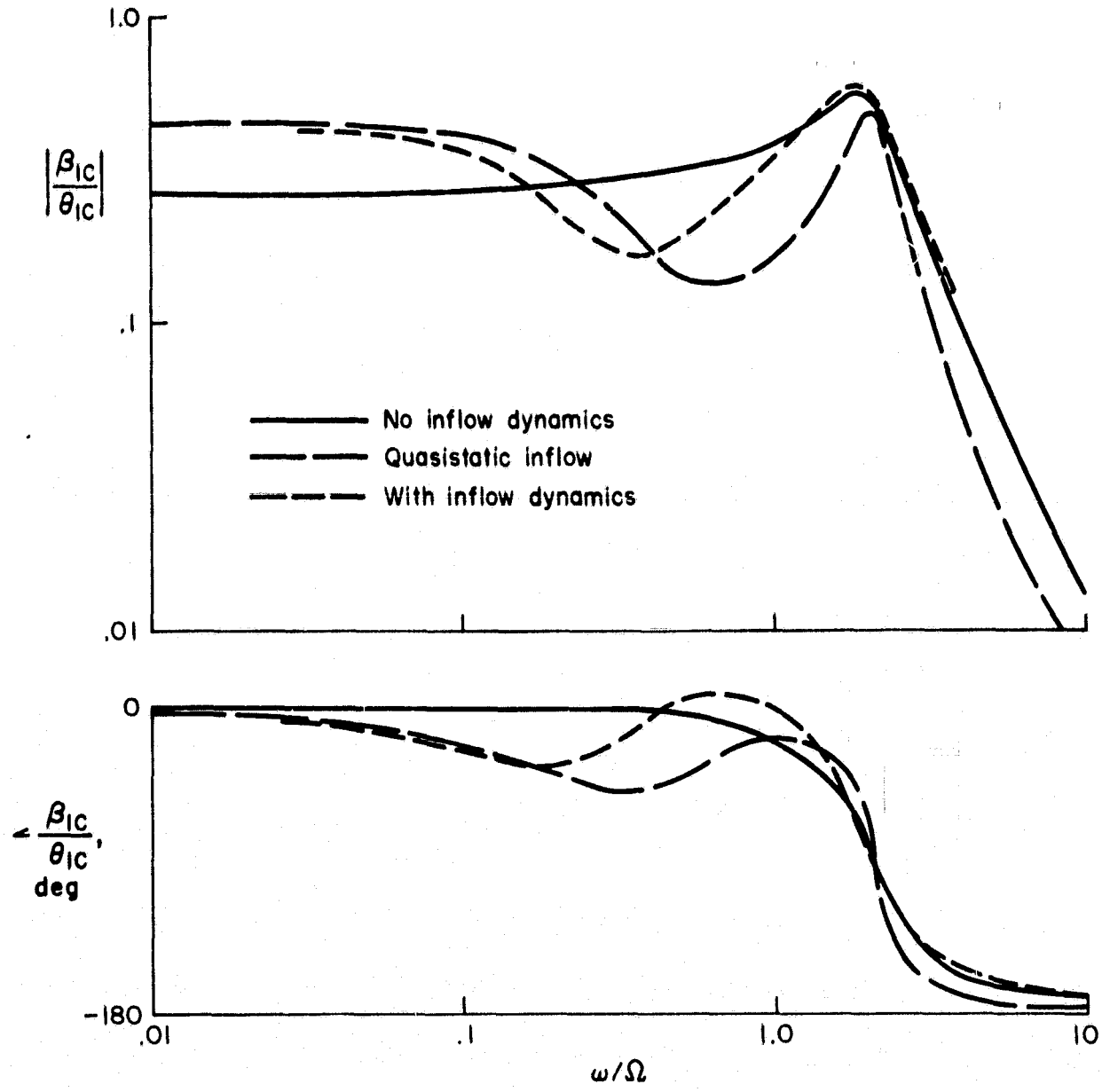

Figure 3. Magnitude and phase of longitudinal tip-path-plane tilt response to lateral control plane inputs (β_{1c}/θ_{1c}) for a hovering, three-bladed hingeless rotor (flap frequency $\bar{\nu} = 1.15$), showing the influence of the inflow dynamics.

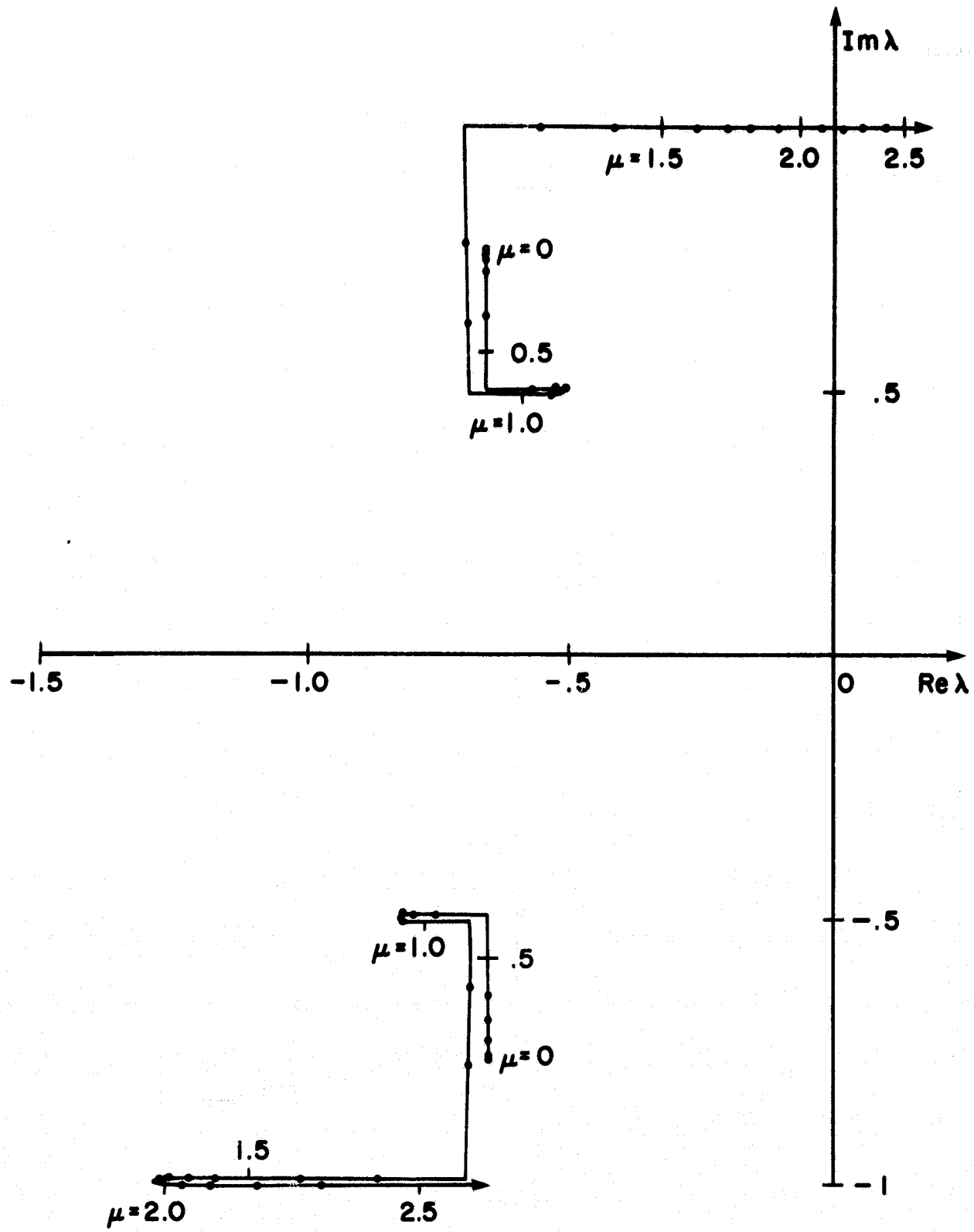

Figure 4. Root locus of forward-flight flapping stability for a single articulated rotor blade (γ = 10, flap frequency ν = 1.0, no pitch/flap coupling).

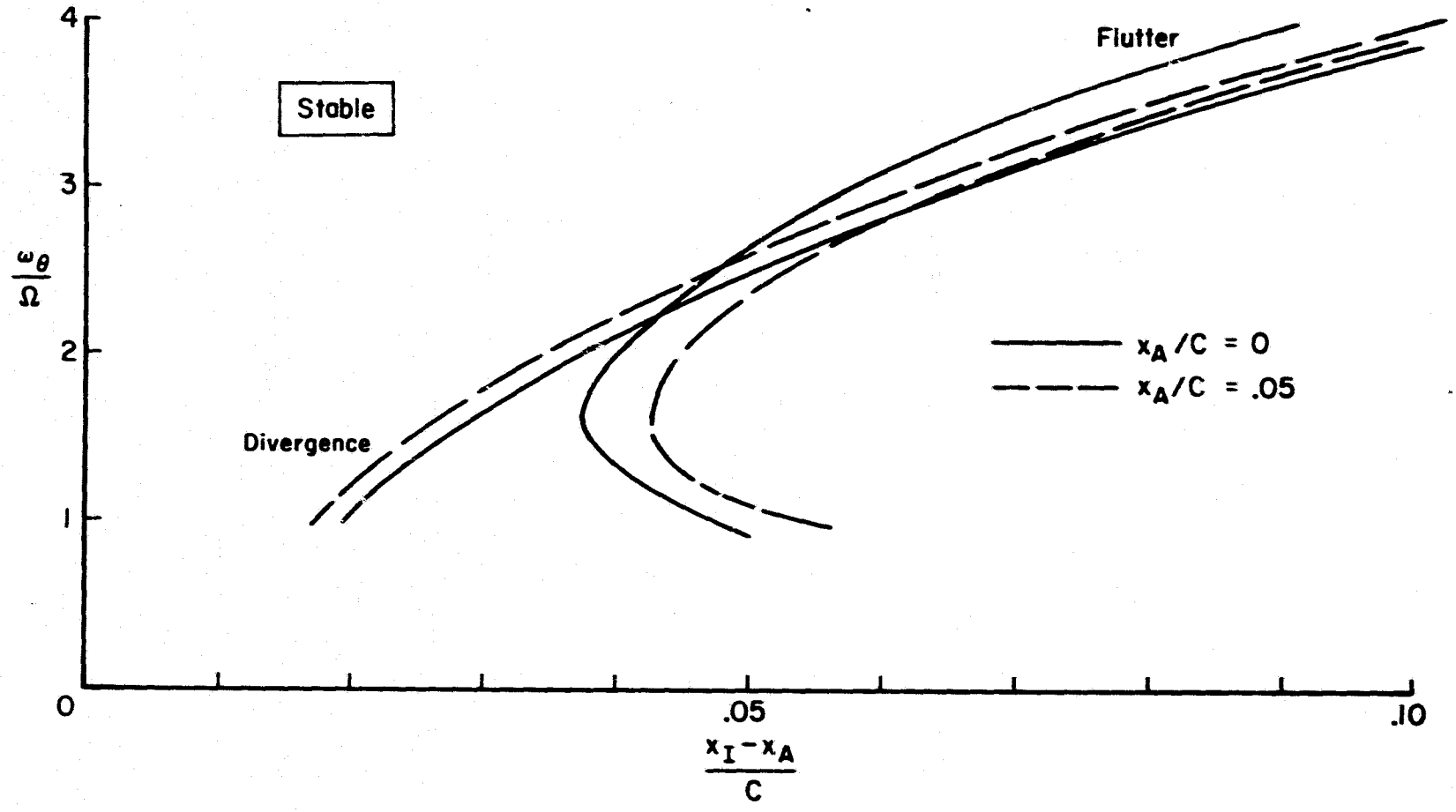

Figure 5. Pitch/flap flutter stability boundaries of an articulated rotor in hover, for $x_A/c = 0$ and .05.

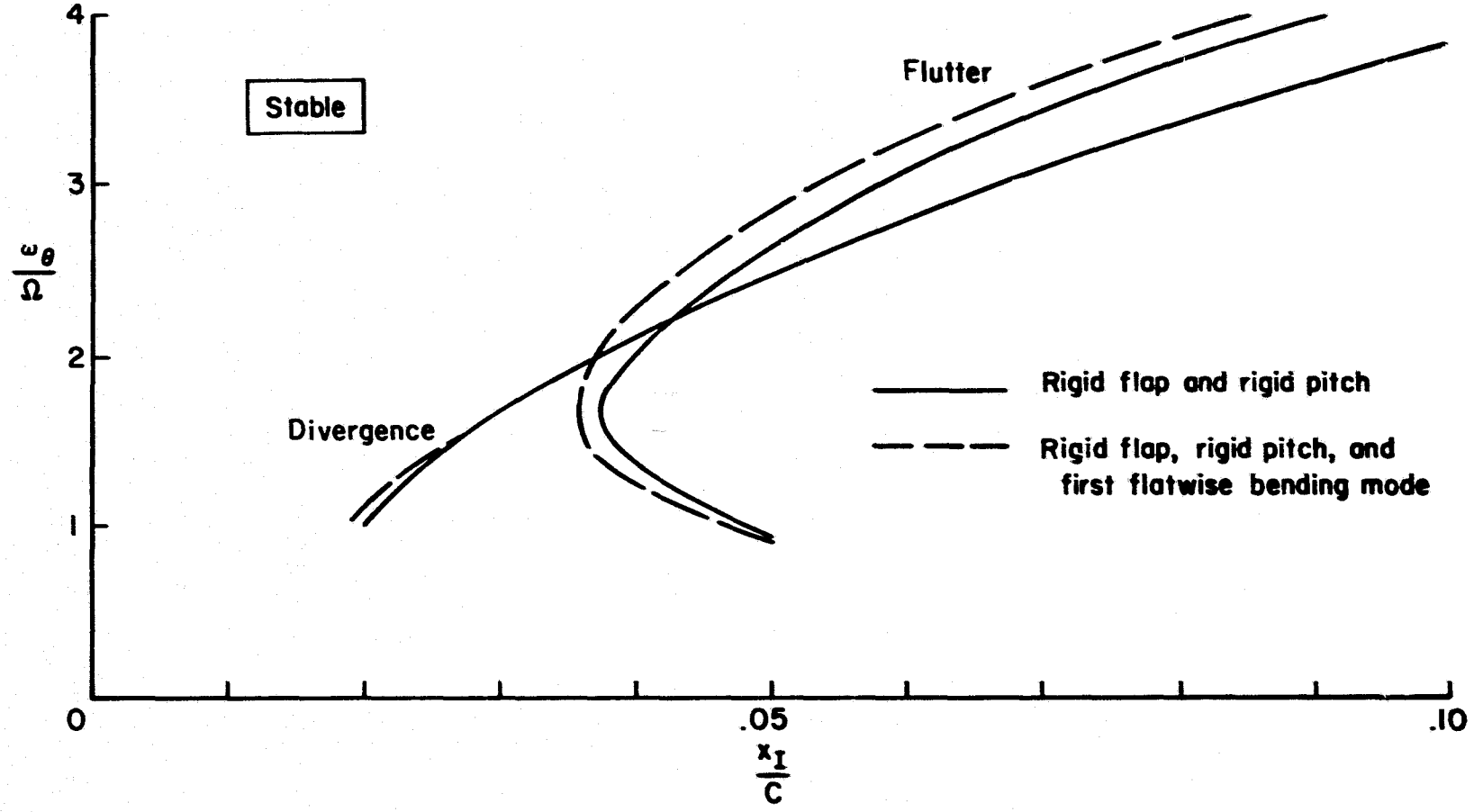

Figure 6. Pitch/flap flutter stability boundaries of a hovering articulated rotor, with and without the first flatwise bending mode.

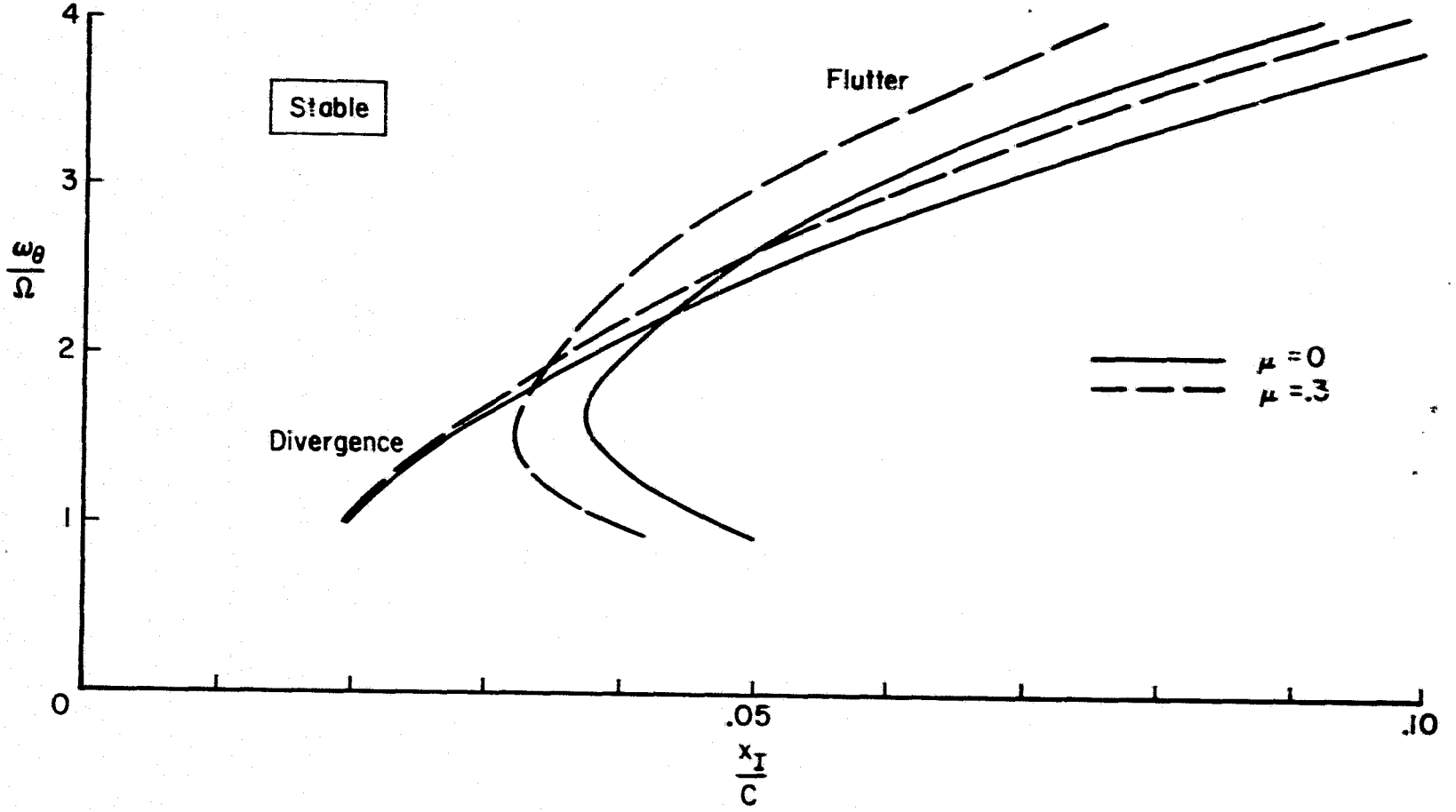

Figure 7. Pitch/flap flutter stability boundaries of an articulated rotor, for $\mu = 0$ and .3 (constant coefficient approximation used for $\mu = .3$ calculations).

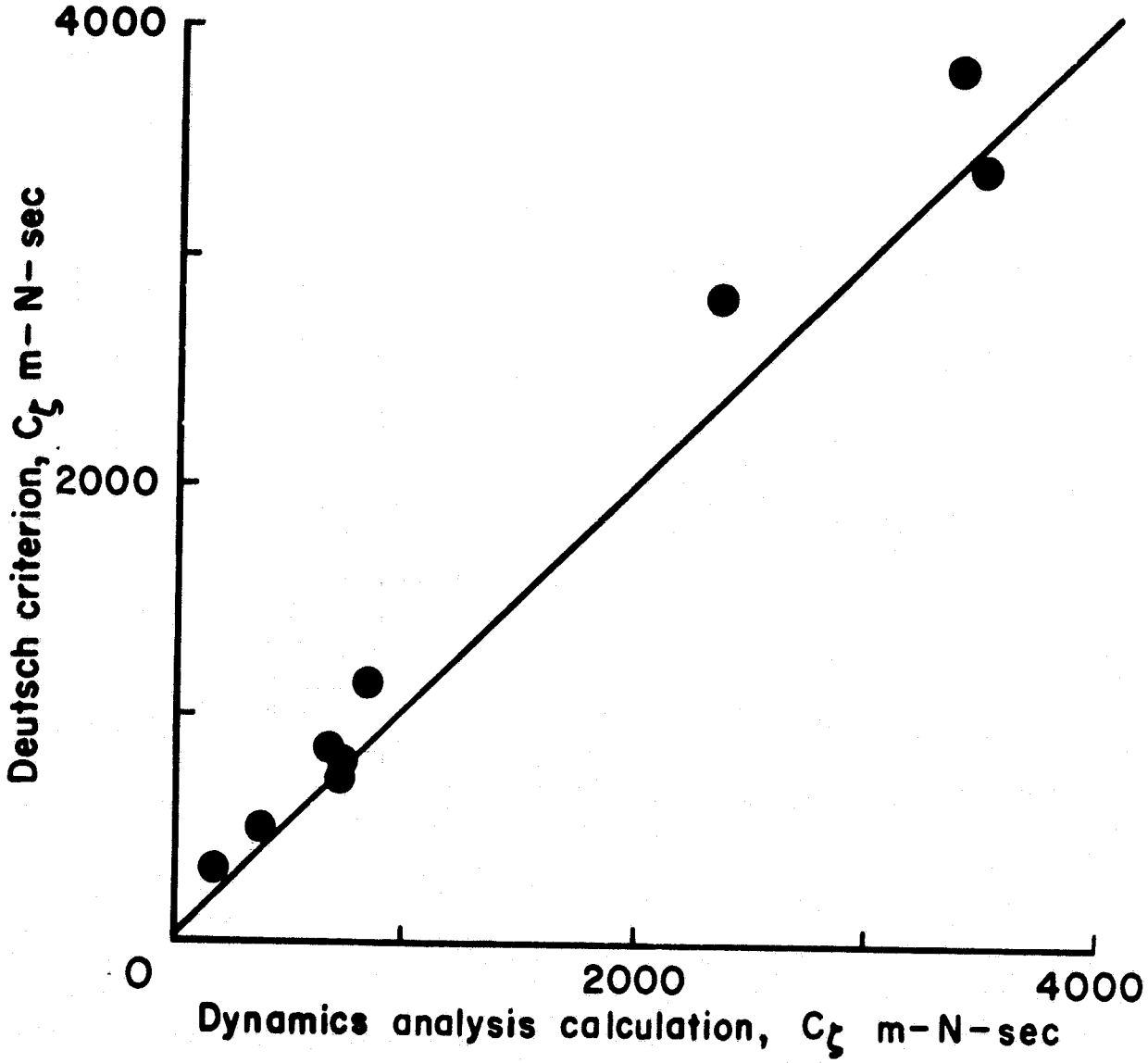

Figure 8. Comparison of blade lag damping at the ground resonance stability boundary, as calculated by the Deutsch criterion and using the dynamics analysis of reference 1.

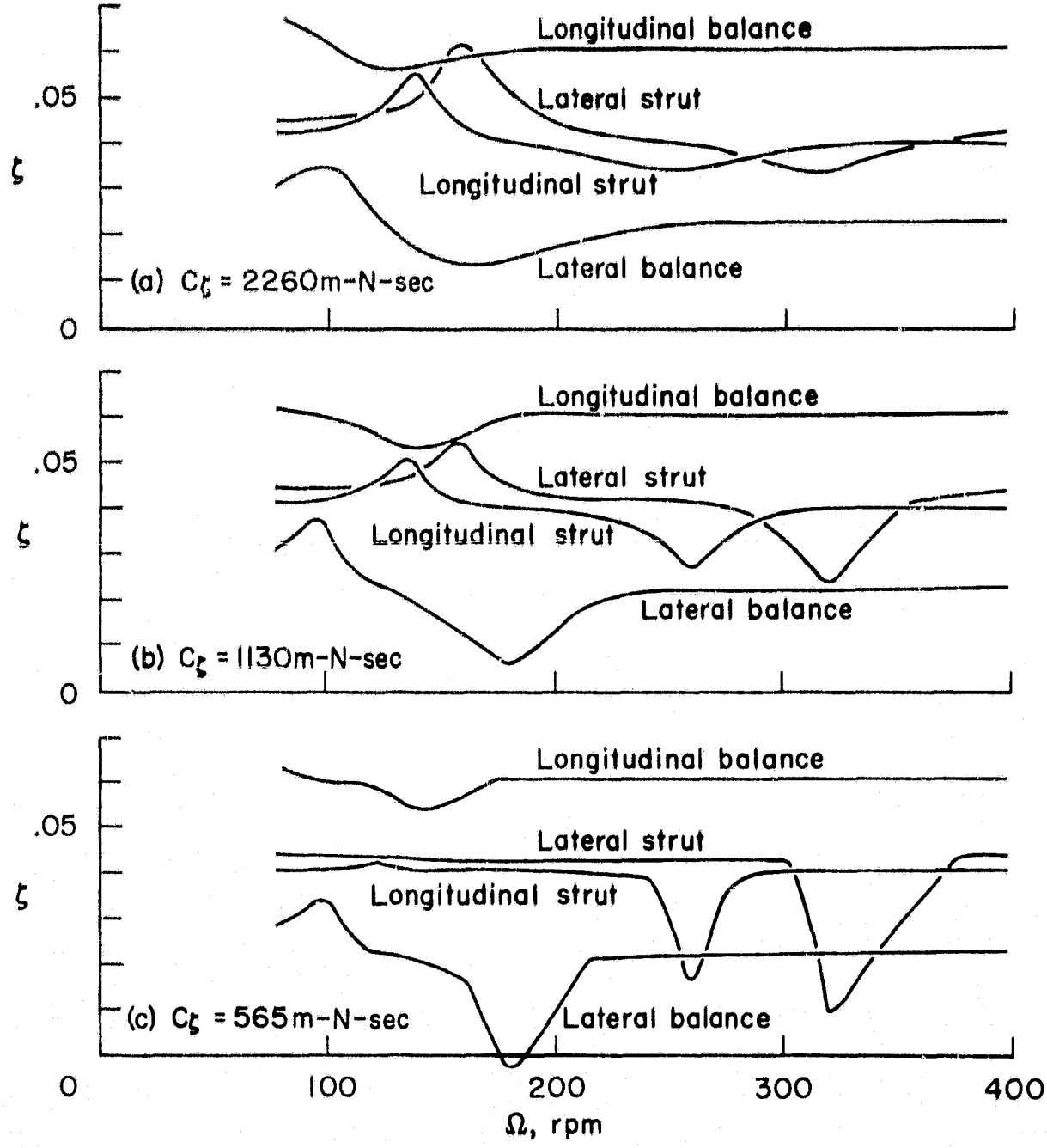

Figure 9. Ground resonance stability calculations for a four-bladed articulated rotor on a wind tunnel strut and balance system: damping ratio of the support modes as a function of rotor speed, for three levels of blade lag damping.